DOI:
10.1016/j.jid.2016.01.036

Document Version
Peer reviewed version

Accepted Manuscript

β-catenin stabilization in skin fibroblasts causes fibrotic lesions by preventing adipocyte differentiation of the reticular dermis

Maria Mastrogiannaki, Beate M. Lichtenberger, Andreas Reimer, Charlotte A. Collins, Ryan R. Driskell, Fiona M. Watt

PII: S0022-202X(16)00489-9

DOI: 10.1016/j.jid.2016.01.036

Reference: JID 192

To appear in: *The Journal of Investigative Dermatology*

Received Date: 23 September 2015

Revised Date: 13 January 2016

Accepted Date: 28 January 2016

Please cite this article as: Mastrogiannaki M, Lichtenberger BM, Reimer A, Collins CA, Driskell RR, Watt FM, β-catenin stabilization in skin fibroblasts causes fibrotic lesions by preventing adipocyte differentiation of the reticular dermis, *The Journal of Investigative Dermatology* (2016), doi: 10.1016/j.jid.2016.01.036.

β-catenin stabilization in skin fibroblasts causes fibrotic lesions by preventing adipocyte differentiation of the reticular dermis

Maria Mastrogiannaki[1, 2, 3], Beate M. Lichtenberger[1, 2, 3], Andreas Reimer[1], Charlotte A. Collins[2], Ryan R. Driskell[1] and Fiona M. Watt[1]*

[1]Centre for Stem Cells and Regenerative Medicine, King's College London, Guy's Hospital, Great Maze Pond, London SE1 9RT, UK

[2] Wellcome Trust Centre for Stem Cell Research, University of Cambridge, Tennis Court Road, Cambridge CB2 1QR, UK

[3] Co-first authors

*Corresponding author: Fiona M. Watt

Email: fiona.watt@kcl.ac.uk

Tel: 020 7188 5608

Key words: skin, fibroblast lineages, fibrosis, adipocyte, β-catenin

Running title: β-catenin regulates fibroblast lineages

ABSTRACT

The Wnt/β-catenin pathway plays a central role in epidermal homeostasis and regeneration but how it affects fibroblast fate decisions is unknown. Here, we investigated the effect of targeted β-catenin stabilization in dermal fibroblasts. Comparative gene expression profiling of Sca1- and Sca1+ neonatal fibroblasts, from upper and lower dermis respectively, confirmed that Sca1+ cells had a pre-adipocyte signature and revealed differential expression of Wnt/β-catenin-associated genes. By targeting all fibroblasts or selectively targeting Dlk1+ lower dermal fibroblasts, we found that β-catenin stabilization between E16.5 and P2 resulted in a reduction in the dermal adipocyte layer with a corresponding increase in dermal fibrosis and an altered hair cycle. The fibrotic phenotype correlated with a reduction in the potential of Sca1+ fibroblasts to undergo adipogenic differentiation *ex vivo*. Our findings indicate that Wnt/β-catenin signaling controls adipogenic cell fate within the lower dermis, which potentially contributes to the pathogenesis of fibrotic skin diseases.

INTRODUCTION

The epidermis is maintained by distinct subpopulations of stem cells whose fate is regulated by intrinsic mechanisms and external signals from the niche (Kretzschmar and Watt, 2014; Lim and Nusse, 2013). Signaling between epidermal stem cells and cells in the underlying dermis is reciprocal (Millar, 2002; Sennett and Rendl, 2012). Such interactions can occur at close range, for example via extracellular matrix deposition (Fujiwara *et al.*, 2011), and by long-range signaling mediated by epidermal secreted factors (Collins *et al.*, 2011; Donati *et al.*, 2014). Furthermore, factors secreted by proliferating adipocyte progenitors (Festa *et al.*, 2011) and differentiated

adipocytes (Plikus and Chuong, 2014; Plikus *et al.*, 2008) regulate the hair growth cycle.

The dermis contains a variety of subpopulations of mesenchymal cells, with different locations and functions (Driskell and Watt, 2015). At E12.5 mouse dermal cells are capable of differentiating into all the different fibroblast types present in postnatal skin. However, at about E16.5 of mouse development, the dermal mesenchyme undergoes commitment to two different lineages. In late embryonic and neonatal skin, the upper dermal lineage gives rise to papillary fibroblasts, the cells of the arrector pili muscle (APM) (responsible for pilo-erection), the dermal sheath and the dermal papilla. The lower dermal lineage gives rise to the reticular fibroblasts, which deposit most of the skin fibrillar collagen, pre-adipocytes and mature adipocytes (Driskell *et al.*, 2013). The different fibroblast lineages are functionally significant, because the upper, papillary lineage is required for new hair follicle formation while the lower (or reticular) lineage is responsible for the first wave of dermal repair following wounding (Driskell *et al.*, 2013). However, the molecular mechanisms that determine fibroblast fate decisions are largely uncharacterized (Driskell *et al.*, 2009).

Epidermal Wnt/β-catenin signaling causes profound changes in the underlying dermis, leading to expansion of both the upper and lower dermal lineages, de novo formation of dermal papillae and an increase in adipocyte differentiation (Collins *et al.*, 2011; Donati *et al.*, 2014; Lichtenberger *et al.*, 2016). In addition, there is compelling evidence that Wnt/β-catenin signaling in fibroblasts regulates the composition of the dermis. β-catenin is necessary and sufficient to specify dermal fate in different body regions during mouse embryonic development (Atit *et al.*, 2006; Ohtola *et al.*, 2008). Wnt/β-catenin signaling has a well-characterized inhibitory effect

on adipogenic differentiation (Gesta *et al.*, 2007; Kennell and MacDougald, 2005; Longo *et al.*, 2004), while being required in the dermal papilla to promote hair follicle formation and control dermal papilla activity and size (Enshell-Seijffers *et al.*, 2010; Kaushal *et al.*, 2015; Tsai *et al.*, 2014). Furthermore, it was shown recently that expression of stabilised β-catenin in fibroblasts of mouse ventral dermis at E16.5 results in progressive skin fibrosis, with thickened collagen fibres and altered collagen fibril morphology (Hamburg-Shields *et al.*, 2015).

In this study, we performed comparative gene expression of distinct populations of neonatal fibroblasts, which revealed differential expression of Wnt pathway genes. Using a conditional targeting approach, we examined the effects of β-catenin stabilization in all fibroblasts or selectively in reticular fibroblasts. Our findings indicate a key role of Wnt/β-catenin signaling in regulating the differentiation of reticular fibroblasts into adipocytes.

RESULTS

Differential expression of adipocyte genes in upper and lower dermal fibroblasts

As previously reported (Collins *et al.*, 2011), in PdgfrαH2BEGFP mice (Hamilton *et al.*, 2003) nuclear EGFP expressed under the control of the Pdgfrα promoter is detected in all dorsal skin fibroblasts (Figure 1a-d). In neonatal (P2) skin, Sca1 is absent from the upper (papillary) dermis but is expressed by reticular fibroblasts, pre-adipocytes and skin adipocytes in the lower dermis (Donati *et al.*, 2014; Driskell *et al.*, 2013; Festa *et al.*, 2011). Immunolabeling confirmed that the majority of reticular fibroblasts express Sca1 at P2 (Figure 1c, d). We have previously demonstrated that

fibroblasts that express Dlk1 at E16.5 give rise to the Sca1+ fibroblasts and mature adipocytes present in P2 and adult skin, although Dlk1 is no longer expressed in adult skin (Driskell *et al.*, 2013; Lichtenberger *et al.*, 2016). To compare fibroblasts from the upper and lower dermis, we therefore sorted EGFP+ cells from P2 dorsal dermis and fractionated the cells further on the basis of Sca1 surface marker expression (Figure 1e). We also sorted EGFP-/Sca1- cells as a control.

Q-PCR analysis of mRNA isolated from the different dermal subpopulations showed that mRNAs corresponding to *Pdgfra* and the fibroblast marker genes *Col1a2* and *Vimentin* were highly enriched in both PdgfrαEGFP+ subpopulations relative to PdgfrαEGFP- cells (Figure 1f-h), while mRNA corresponding to *Ly6a* (Sca1) was highly enriched in the PdgfrαEGFP+/ Sca1+ fraction (Figure 1i), confirming the relative purity of the sorted cell populations. The adipocyte/pre-adipocyte marker genes *Fabp4*, *Perilipin*, *Pparg* and *Dlk1* (Pref-1) were also enriched in PdgfrαEGFP+/ Sca1+ cells, consistent with previous reports (Driskell *et al.*, 2013; Festa *et al.*, 2011) (Figure 1j-m). The Q-PCR results were confirmed by immunofluorescence labelling of P2 dorsal skin with antibodies to Fabp4 and Perilipin (Figure 1n-q).

Differential expression of Wnt pathway genes in upper and lower dermal fibroblasts

To explore the differences between PdgfrαEGFP+/ Sca1+ and PdgfrαEGFP+/ Sca1- fibroblasts, we carried out gene expression profiling using RNA from flow-sorted cells. 1,457 entities were regulated by >2-fold (t test, $p<0.05$) (Figure 2a; Table S1), demonstrating that global differences in gene expression distinguish the two fibroblast subpopulations. In addition to differential expression of adipogenic genes,

there was differential expression of genes encoding zinc finger proteins (Gupta *et al.*) and regulators of the Wnt, BMP, Notch and PDGF signaling pathways (Figure 2b, c).

Since Wnt/β-catenin signaling is known to regulate dermal development, differential expression of genes associated with this pathway was of particular interest (Figure 2c). Several Wnt/β-catenin pathway genes were differentially regulated in PdgfrαEGFP+/ Sca1+ and PdgfrαEGFP+/ Sca1- fibroblasts, which we confirmed by Q-PCR in independent biological samples (Figure 2d-j). PdgfrαEGFP+/ Sca1+ fibroblasts expressed significantly lower levels of *Wnt5a* ligand, the Wnt receptor *Frzb* and the Wnt effector *Lef1*, as well as several other Wnt regulatory genes including *Axin2* and *Dkk1* (Figure 2d-h; see also Driskell *et al*., 2013). However, Sca1+ cells expressed significantly higher levels of the Wnt receptor *Fzd4* and the Wnt effector *Tcf7l2* (Figure 2i, j). Tcf7l2, commonly known as TCF4, is expressed in human adipose tissue, and gene variants are associated with susceptibility to Type 2 diabetes and inability to lose weight following lifestyle interventions (Cauchi *et al.*, 2006; Haupt *et al.*, 2010). There was no significant difference in β-catenin mRNA levels in PdgfrαEGFP+/ Sca1- and PdgfrαEGFP+/ Sca1+ fibroblasts at P2 (Figure 2k). However, immunostaining revealed differential protein expression of β-catenin in upper and lower dermis of neonatal skin, with high levels of nuclear β-catenin in papillary fibroblasts and only few nuclear β-catenin positive cells within the adipose tissue (Fig. 2l, m, o, p).

Consistent with the microarray and Q-PCR data, immunostaining of neonatal skin with antibodies recognizing Tcf3/4 and Lef1 revealed that Tcf3/4 localized to the lower reticular dermis (PdgfrαEGFP+/ Sca1+) while Lef1 stained the upper papillary

dermis (PdgfrαEGFP+/ Sca1-) (Figure 2n, q, r). However, there were some scattered cells in the lower dermis that co-expressed Tcf3/4 and Lef1 (white arrow heads).

We conclude that neonatal dermis is compartmentalized such that Wnt/β-catenin signaling pathway components are differentially expressed in Sca1+ and Sca1- fibroblasts.

Constitutive β-catenin stabilization in postnatal skin fibroblasts reduces the adipocyte layer and disturbs the hair growth cycle

Given the inhibitory effect of Wnt/β-catenin signaling on adipogenic differentiation (Gesta *et al.*, 2007; Kennell and MacDougald, 2005; Longo *et al.*, 2004), we speculated that activating the pathway in postnatal skin fibroblasts would change the composition of the dermis by altering neonatal fibroblast lineage fate or differentiation. In order to determine the effect of active Wnt/β-catenin signaling in all neonatal fibroblasts, we produced crosses between PdgfraCreER^{T2} (Rivers *et al.*, 2008) and Ctnnb1 Exon3$^{Flox/+}$ (Harada *et al.*, 1999) mouse strains. Recombination of Ctnnb1 Exon3$^{Flox/+}$ (referred as cΔex3) produces a variant of β-catenin that is resistant to phosphorylation by Glycogen Synthase Kinase 3β (GSK3β) and degradation by the Adenomatous Polyposis Complex (APC). Littermates were treated topically with 4-hydroxy-tamoxifen (4-OHT) on the day of birth and analyzed at different time points thereafter (Figure 3a).

By generating triple transgenics through crossing PdgfraCreER^{T2}, Rosa-CAG-LSL-TdTomato (TdTomato-LSL) and Ctnnb1 Exon3$^{Flox/+}$ mice, we could demonstrate equal recombination efficiency whether or not β-catenin was stabilized. 50-60% of all

PDGFRα+ fibroblasts were Tdtomato+ at P4 in control and mutant (cΔex3) littermates (Figure 3b; Figure S1a). TdTomato+ cells isolated from back skin at P4 did not express α6 integrin (a marker of epidermal keratinocytes), CD31 (endothelial cell marker), CD45 or other markers of haematopoietic lineages (Figure S1a and data not shown). The recombination efficiency was similar in different fibroblast subpopulations (Figure 3b). Lrig1+/Sca1- cells are resident in the papillary dermis; Dlk1+/Sca1- cells are a subpopulation of P2 reticular fibroblasts; Sca1+ cells, which can be Dlk1+ or Dlk1-, are found in the lower dermis and subdermal fat layer (Driskell *et al.*, 2013). Analysis of skin sections confirmed that TdTomato+ cells were present in all dermal layers (Figure 3c, d). Importantly, a high abundance of nuclear β-catenin was detected in Tdtomato+ fibroblasts of cΔex3 skin at P4 (Figure S1c-f) and was even more pronounced at P56 (Figure 3e-h). Furthermore, Q-PCR revealed increased (albeit not significant) expression levels of known Wnt/β-catenin target genes such as *Nov*, *Sp5* and *Gpr165* (Hamburg-Shields *et al.*, 2015) in flow sorted Tdtomato+ fibroblasts isolated from mutant skin compared to control skin (Figure S1g) at P4. Interestingly, at P56 expression levels of Nov were similar in TdTomato+/Sca1- fibroblasts in wild-type and mutant dermis but significantly upregulated in TdTomato+/Sca1+ fibroblasts, thereby reaching similar levels between papillary and reticular fibroblasts (Figure S1h).

No differences in skin morphology were observed between mutant and control mice at P4 (Figure 3i, j). However, at P18 we observed fibroblast-rich regions within the adipocyte layer of cΔex3 mice (Figure 3k, l). At P35 these fibrotic regions were prominent (Figure 3m, n), and at P56 the adipocyte layer had been largely replaced by fibrotic dermis (Figure 3o, p).

To assess whether Wnt/β-catenin signaling in fibroblasts affects the hair cycle we classified different stages of hair follicles (HF) according to their morphology (Muller-Rover *et al.*, 2001; Paus *et al.*, 1999) and also examined their length. For each time point we examined at least 8 HF per skin sample and skin biopsies from 2-8 different mice of the same genotype. We examined skin at P4 and P11 (n=3-4), during the growth phase of HF morphogenesis; P18 (n=3-5), P24 (n=2-4) and P28 (n=2), during the first postnatal telogen; P35 (n=6), anagen; and P42 (n=4-8) and P56 (n=3-6), when the follicles are entering catagen and the second telogen, respectively. Regardless of genotype and age all HF were synchronized, with the exception of P35 cΔex3 mice, when 2/8 mice were still in telogen while the others were in anagen. Hair follicle morphogenesis occurred normally in cΔex3 mice (day 4 and 10; Figure 3q, r), as did the first telogen (day 18) and first anagen (day 35; Figure 3q, r). However, from day 42 the hair cycle was disturbed in both male (Figure 3q) and female (Figure 3r) cΔex3 mice, and cΔex3 follicles remained in anagen, as assessed both by morphology and length, when wildtype follicles were entering telogen (Figure 3o-r). Based on the observation that in 2/8 mutant mice HF were still in telogen at P35, which were not scored in (Figure 3m, n), we speculate that there may be an extended growth phase prior to the second catagen. This is supported by the observation that there was an increased number of proliferating phosphoHistone H3+ cells in the outer root sheath (ORS) of HF in mutant mice (Figure 3s). Nevertheless, HF in mutant skin eventually entered catagen, and all HF were in telogen at the age of 3 months (n=4; Figure S1i, j). Thus, our findings indicate that fibroblast-specific β-catenin stabilizationperturbs the hair cycle and extends anagen.

Constitutive β-catenin activation results in dermal fibrosis

To characterize the effect of activated Wnt/β-catenin signaling in fibroblasts, we focused on P35 skin (Figure 4). The fibrotic areas within the adipose layer of cΔex3 dermis labelled pink with the histochemical Herovici stain, indicative of the mature fibrillar collagen (Collins *et al.*, 2011) (Figure 4a, b). Q-PCR revealed reduced expression of differentiation markers such as Fabp4, Perilipin and Cebpα (Figure 4c) in mutant TdTomato+/Sca1+ fibroblasts compared to controls. Immunostaining confirmed reduced protein expression of Perilipin and Fabp4 but revealed higher levels of the pre-adipocyte marker Cd24 (Figure 4 d-i). The reduction in the number of differentiated adipocytes was confirmed by LipidTox staining (Figure 4j, k) and was statistically significant (Figure 4l). Fibroblast proliferative activity, measured by EdU labelling, was increased in both the adipocyte layer and in the rest of the dermis, including papillary fibroblasts of the dermal sheath and reticular fibroblasts, the effect being most pronounced in the adipocyte layer (Figure 4m-o). However, we did not detect significant numbers of EdU+ DP cells, consistent with our previous finding that the number of proliferating cells in adult DP is very low, even when β-catenin is stabilized and the DP increases in size (Kaushal et al., 2015).

Selective Wnt/β-catenin stabilization in Dlk1+ fibroblasts results in fibrosis within the adipose layer

Given the differential expression of adipogenic genes in Sca1+ and Sca1- fibroblasts at P2 (Figure 2) and the fibrosis within the adipose layer on fibroblast-specific stabilization of β-catenin (Figure 3), we hypothesized that the fibrotic effect of activating Wnt/β-catenin signaling in all Pdgfrα+ fibroblasts would be reproduced by selectively targeting the lower dermal lineage during skin development. Since fibroblasts that express Dlk1 at E16.5 give rise to the Sca1+ fibroblasts and mature

adipocytes present at P2 and in adult skin (Driskell *et al.*, 2013), we crossed Ctnnb1 Exon3$^{lox/+}$, Dlk1CreER^{T2} and TdTomato-LSL mice and treated them with tamoxifen at E16.5 to target the lower dermal lineage (Figure 5a).

When fibroblasts were isolated at E18.5, two days after tamoxifen injection in utero, 3% of total (Pdgfrα+) fibroblasts were labelled (Figure 5b; Figure S1b). 10-15% of Dlk1+/Sca1- and Dlk1+/Sca1+ cells were labelled, compared with 2% of Dlk1-/Sca1+ cells (Figure 5b; Figure S1b) and 1% Lrig1+ papillary fibroblasts, confirming the selectivity of targeting. TdTomato+ fibroblasts comprised 30% Dlk1+/Sca1-, 55% Dlk1+/Sca1+ cells and 10% Dlk1-/Sca1+ cells (Fig. 5c). We speculated that TdTomato+ cells within the Dlk1-/Sca1+ fibroblast population correspond to cells that were Dlk1+ at E16.5 but subsequently downregulated Dlk1 expression (Driskell *et al.*, 2013). When examined at P56, TdTomato+ cells were confined to the lower dermis in both control and Dlk1LTΔex3 skin (Figure 5d, e). In control skin the majority of TdTomato+ cells had the morphology of mature adipocytes, whereas in Dlk1LTΔex3 skin the TdTomato+ cells had a fibroblastic morphology (Figure 5d, e; mature adipocytes are labelled with asterisks in Fig. 5d).

In contrast to the effect of activating Wnt/β-catenin signaling in all fibroblasts, selective activation in Dlk1+ cells did not disturb the hair cycle and at P56 both control and cΔex3 skin was in telogen, (Figure 5f, g). Nevertheless, there was an accumulation of fibroblasts within the adipose layer in Dlk1LTΔex3 skin (Figure 5f, g). These regions stained positively for fibrillar ECM using Herovici dye (Figure 5h, i) and expressed high levels of β-catenin (Figure 5j, k). The reduction in adipocyte numbers was confirmed by labelling for caveolin-1, a marker for pre-adipocytes and

adipocytes (Figure 5l, m), and was statistically significant, in accordance with the appearance of fibrotic lesions (Figure 4n, o). Stabilization of β-catenin via Dlk1CreER^{T2} also resulted in an increase in fibroblast proliferation both in the adipocyte layer and in the remaining dermis (Fig. 5p-r).

Postnatal Wnt/β-catenin stabilization inhibits adipogenesis of Sca1+ fibroblasts in culture

To establish whether β-catenin stabilization within pre-adipocytes resulted in an inhibition of differentiation, we analyzed the behaviour of single cells captured in ECM-functionalized hydrogels, as described previously (Driskell *et al.*, 2012; Driskell *et al.*, 2013). PdgfrαCreER^{T2}, TdTomato-LSL and Ctnnb1 Exon3$^{lox/+}$ mice were crossed and treated with tamoxifen on the day of birth (Figure 6a). Sca1+ TdTomato+ fibroblasts were isolated by flow cytometry 2 days later (Figure 6b, c). Activation of Wnt/β-catenin signaling did not affect the proportion of Sca1+ cells that expressed the pre-adipocyte marker Cd24 (Festa *et al.*, 2011) (Figure 6d).

Sca1+ cells were encapsulated at clonal density in 3-dimensional hydrogels and cultured in control or adipogenic medium. After 10 days in culture, individual clones were scored for cell number and the total intensity of LipidTox staining (Figure 6e). Whereas β-catenin stabilization *in vivo* stimulated proliferation within the adipose layer (Figure 4m), there was no effect on clone size when Sca1+ cells were cultured in adipogenic medium, and in standard medium the only effect was to increase the percentage of 2 cell clones at the expense of clones with higher cell numbers (Figure 6f, g). Wnt/β-catenin signaling activation did, however, decrease adipocyte differentiation, as evaluated by decreased LipidTox staining, both in standard

medium (Figure 6h) and in medium supplemented with adipogenic factors, regardless of clone size (Figure 6i). These findings suggest that the effect of β-catenin stabilization in neonatal fibroblasts is to prevent Sca1+ fibroblasts from undergoing adipocyte differentiation in a cell-autonomous manner, rather than changing the proportion of Cd24+/Sca1+ pre-adipocytes.

DISCUSSION

Here we have examined the effect of dermal Wnt/β-catenin signaling in the context of fibroblast heterogeneity. We show that expression of Wnt pathway genes such as Wnt5a, Lef1, Tcf4 or Dkk1 differs between upper (Sca1-) and lower (Sca1+) dermis. Interestingly, immunostaining revealed that β-catenin and Lef1 are more abundant in Sca1- cells. β-catenin stabilization in all fibroblast populations in neonatal skin resulted in a decrease in mature adipocytes and the appearance of fibrotic regions in the adipose layer, accompanied by stimulation of fibroblast proliferation throughout the dermis. The replacement of adipocytes by ectopic reticular fibroblasts also occurred when the lower dermal lineage was selectively targeted at E16.5, prior to adipocyte differentiation.

Our *in vitro* studies revealed that β-catenin stabilization did not drive fibroblast proliferation cell-autonomously. The effect of β-catenin stabilization was to inhibit terminal differentiation of Sca1+ cells rather than to promote expansion of pre-adipocytes or selective proliferation of reticular fibroblasts. This is similar to the effect of β-catenin stabilization on cultured human keratinocytes, which is to expand the stem cell compartment without stimulating proliferation (Zhu and Watt, 1999). However, although we did not detect an expansion of pre-adipocytes within 4 days of

β-catenin stabilization *in vivo*, Cd24 expression was increased in P35 skin, which could either be due to an expansion of pre-adipocytes at a later stage, which is supported by increased fibroblast proliferation *in vivo*, or a secondary effect of the differentiation defect.

Our conclusion that targeting the lower dermal lineage accounts for the appearance of fibrotic regions is consistent with other studies highlighting the contributions of different dermal cell subpopulations to fibrosis. For example, fibroblasts that express Engrailed 1 during development are responsible for the bulk of extracellular matrix deposition in dorsal dermis and mediate dermal fibrosis in response to irradiation (Rinkevich *et al.*, 2015). Other dermal subpopulations that contribute to fibrosis include Sox2+ cells (Liu *et al.*, 2014) and adiponectin-positive adipocyte precursors (Marangoni *et al.*, 2015). In addition, Adam12+ perivascular mesenchymal cells expressing PDGFRα and Sca1 are pro-fibrotic in response to injury (Dulauroy *et al.*, 2012).

The inhibition of adipocyte differentiation was not the only effect of dermal β-catenin that we observed. There was an increase in proliferation throughout the dermis, consistent with an earlier report (Cheon *et al.*, 2002) and a disruption of the hair follicle cycle. The effects on the hair cycle cannot be attributed solely to a decrease in mature adipocytes (Donati *et al.*, 2014; Festa *et al.*, 2011) because they were observed when we targeted all fibroblast subpopulations via PdgfraCreER^{T2} and not when we selectively targeted the lower dermal lineage. This raises an interesting question as to whether increased proliferation of the fibroblast subpopulations that

are known to regulate hair growth, in particular the dermal papilla, dermal sheath and other papillary fibroblasts (Driskell *et al.*, 2013; Enshell-Seijffers *et al.*, 2010; Kaushal *et al.*, 2015), is responsible. We have previously shown that β–catenin stabilization in Prominin-1 expressing DP cells results in an increase DP size, but since the number of EdU+ cells is very low the increase could be attributable to a number of factors, such as increased migration from the dermal sheath (Kaushal *et al.*, 2015). Since the PdgfrαCreER^{T2} transgene is active in DP cells (Figure 3g, h), it is possible that the perturbed hair cycle reflects, at least in part, Wnt/β-catenin activation in DP cells. The effect of β-catenin stabilization on proliferation in the upper and lower dermis could either be direct or indirect, via the dermal extracellular matrix, since Tcf-mediated transcription of several extracellular matrix protein-coding genes has recently been demonstrated in a fibrosis model of sustained β-catenin activity in Hoxb2 derived ventral fibroblasts (Hamburg-Shields *et al.*, 2015).

Our findings are in good agreement with previous reports that β-catenin plays a role in skin fibrosis (Beyer *et al.*, 2012) and causes a downregulation of adipogenic effector pathways, such as cEBP/PPARγ, in culture (Gesta *et al.*, 2007). In addition, expression of the Wnt inhibitor Dkk1 interferes with pro-fibrotic signaling (Akhmetshina *et al.*, 2012). Together, these studies suggest that pharmacological modulation of Wnt signaling could be beneficial in the treatment of skin fibrotic diseases, including scleroderma (Ohgo *et al.*, 2013). Similar mechanisms could also be responsible for the regulation of mesenchymal progenitors in other organs, including PDGFRα+/Sca1+ muscle fibroblasts with proliferative and myofibroblast/ adipogenic potential in response to muscle regeneration and ectopic fat formation (Uezumi *et al.*, 2010).

MATERIALS & METHODS

***In vivo* experiments** The following mouse strains were maintained on a C57 Bl6/CBA background: Dlk1CreER^{T2} (ICS), PdgfrαEGFP (PdgfrαH2B-eGFP) (Jackson Laboratories), Ctnnb1lox(ex3)/+ (Harada *et al.*, 1999). PDGFRαCreER^{T2} (Rivers *et al.*, 2008) and Rosa-CAG-LSL-TdTomato (Jackson Laboratories; 007905) strains were maintained as homozygotes. Cre-mediated recombination was induced by topical application of 2mg 4-hydroxy-tamoxifen (4-OHT) (Sigma; diluted in acetone +10% DMSO) on the back skin of neonatal pups at P0-P1. For lineage tracing experiments, plugged females received a single intraperitoneal injection of 25µg tamoxifen per g body weight at E16.5. Tamoxifen was dissolved in corn oil (10-20mg/ml) by intermittent sonication at 37℃ for 20- 30 minutes. Pups were harvested and fostered after surgical removal between E18.5-E21. For in vivo proliferation assays, mice received a dose of 500µg 5-ethynyl-2'-deoxyuridine (EdU; 2.5mg/mL in PBS) by intraperitoneal injection 2-4 hours prior to sacrifice. Cohorts included male and/or female littermates and results are representative of at least 3 biological samples. All experimental procedures were carried out under the terms of a UK Home Office project license following ethical review at Cambridge University or King's College London.

Histology

Skin samples were harvested and processed to generate paraffin (5µm) or thick cryo-preserved wholemount tissue sections (50-100µm) as previously described (Collins *et al.*, 2011; Driskell *et al.*, 2013). Immunostaining was performed using the following antibody combinations: rabbit anti-Rfp (1:300; Rockland)/ rabbit anti-Perilipin 1A

(1:100; Abcam)/ rabbit anti-Caveolin-1 (1:100; Abcam); rabbit anti-Fabp4 (1:100; Abcam); donkey anti-rabbit Alexa Fluor 555, 594 or 488; goat anti-PDGFRα and goat anti-Sca1 (1:100; R&D Systems), donkey anti-goat Alexa Fluor 488 or 647; chicken or rabbit anti-Keratin 14 (1:100; Covance), goat anti-chicken Alexa Fluor 647 or 555, mouse β-catenin (1:100; BD Transduction), donkey anti-mouse Alexa Fluor 594 or 488; rabbit anti-TCF3/4 (1:100; Abcam) and anti-Lef1 (1:100; Cell Signalling); Alexa Fluor 488 conjugated anti-Cd24 (1:300; BD Pharmingen). LipidTox (1:500 in PBS; Invitrogen) was used to stain neutral lipids in adipocytes. ProLong Gold anti-fade reagent (Invitrogen) or glycerol was used for mounting slides or whole-mount sections, counterstained with 4', 6-diamidino-2-phenylindole (DAPI). The EdU click-it imaging kit (Invitrogen) was used for detecting incorporated EdU nucleoside analogs in proliferating cells. Herovici staining was performed as previously described (Collins *et al.*, 2011).

Image acquisition and quantification

Immunostained tissue sections were imaged using a Nikon A1R confocal microscope. Adobe Photoshop CS6 was used to adjust images and correct background. Bright field images were collected using either a Hamamatsu NanoZoomer slide scanner or a Zeiss Axiophot microscope with a 10x objective and an AxioCam HRc camera. Image measurements were performed on at least 6 microscopic fields per biological sample.

Cell isolation and flow cytometry

Dermis was separated from back skin of embryos (E18.5-E19.5) or postnatal pups (P2-P4) by incubation with thermolysin (0.25 mg/ml) (Sigma T7902) overnight at 4°

C, digested in DMEM + 10% FBS containing 2.5 mg/mL collagenase I (Gibco 17100-017), and further processed as previously described (Collins *et al.*, 2011). Cells were labeled in PBS + 10% FBS TruStain fcX anti-mouse blocking buffer with the following antibodies: anti-mouse Ly-6A/E (Sca-1)-Alexa Fluor 488, 700 or BV605 (clone D7; 1:200), CD140a/ Pdgfra-APC (clone APA5; 1:20), CD45-Alexa Fluor 700 (clone 30-F11; 1:100), CD24-Fitc (Clone M1/69; 1:100) (eBioscience), Lrig1-Alexa Fluor 488 (polyclonal; 1:20) (RnD Systems), anti-rat Dlk1-Fitc (clone 24-11; 1:20) (MBL International), anti-mouse-CD31-Alexa Fluor 647 (BD Pharmingen), APC Mouse Lineage Antibody Cocktail (BD Pharmingen), and anti-human CD49f-Alexa Fluor 647 (clone NKI-GoH3; 1:20) (Serotec). A BD LSRFortessa™ was used for flow cytometry and an Aria II for sorting fibroblasts. Dead cells were excluded from analysis using DAPI. Fibroblasts were either sorted for CD140α expression or negatively selected by excluding epidermal, endothelial and immune cells from the cell suspension (ITGA6-/LIN-/CD31-). Data analysis and visualization was performed using FlowJo software version 7.6.5.

Hydrogel culture and high-content imaging

Sorted fibroblasts were collected and encapsulated in Extracel (Glycosan Biosystems) as previously described (Driskell *et al.*, 2012), at a density of 5 x 10^5 per ml in µClear 96-well plates (Corning). Cultures were maintained for 10 days at 37°C/ 5% CO_2 in standard medium (DMEM + 10% FBS + 1% penicillin/streptomycin) or Adipogenic medium (StemXVivo Osteogenic/Adipogenic Base Media with Adipogenic Supplement; R&D Systems), and the medium was changed every 2-3 days.

Cultures were fixed with 4% paraformaldehyde for 10 minutes, washed twice in PBS, permeabilized with 0.1% Triton X-100 for 5 minutes and stained with LipidTox, DAPI and rabbit anti-Rfp (1:300 dilution). Multiple image stacks of each colony were recorded using the Operetta High Content Imaging system (Perkin Elmer). Spheres were identified by staining for TdTomato and the number of nuclei per sphere was determined using quantification algorithms on the Colombus analysis software. The fluorescence intensity of LipidTox staining was measured for each sphere.

Quantification and Statistics

GraphPad Prism 6 software was used for all analysis of numerical data, generation of graphs and statistical tests, including one-way ANOVA or student's t-test. Error bars represent standard error of the mean (SEM).

Microarray

Genome-wide expression profiling was carried out by the Paterson Institute Microarray Core Facility, as described previously (Collins *et al.*, 2011). The data are deposited in the NIH GEO repository under accession number GSE76751. cDNA was hybridized to Affymetrix MG430.2A arrays. Array images produced by the Affymetrix PICR 3000 scanner were imported as CEL files into Genespring GX11 (Agilent) for analysis. RMA normalization (baseline to median of all samples) was used. Analyses were performed on genes selected for expression above the bottom 20th percentile in all three samples within at least one of two experimental groups. To identify differentially expressed genes, we compared the two groups using the Student's t- test (p value cut off 0.05). Entities regulated by >2 fold were selected for further analysis.

CONFLICT OF INTEREST

The authors declare no competing financial interests.

ACKNOWLEDGEMENTS

This work was supported by grants to F.M.W. from the Medical Research Council, and the Wellcome Trust. M.M and B.M.L were supported by long-term post-doctoral fellowships by European Molecular Biology Organization (EMBO) (M.M) and Federation of European Biochemical Societies (FEBS) (B.M.L). We gratefully acknowledge excellent support from staff at King's College London and Wellcome Trust Centre for Stem Cell Research, particularly J. Harris, Head of the Nikon Microscopy Centre at King's. We gratefully acknowledge financial support in the form of access to the Biomedical Research Centre flow cytometry core in Guy's & St Thomas' NHS Foundation Trust.

AUTHOR CONTRIBUTIONS

M.M and B.M.L. equally contributed to performing and analyzing the experiments in Figures 2, 3, 4, 5 and 6. A.R. performed and analyzed experiments in Figure 6. C.A.C. generated and analyzed the microarray data, which were validated by R.R.D., and generated data in Figures 1 and 2. F.M.W. contributed to experimental design and analysis. M.M., B.M.L. and F.M.W. wrote the manuscript. All authors contributed to interpreting the findings and editing the final manuscript.

REFERENCES

Akhmetshina A, Palumbo K, Dees C, Bergmann C, Venalis P, Zerr P*, et al.* (2012) Activation of canonical Wnt signalling is required for TGF-beta-mediated fibrosis. *Nat Commun* 3:735.

Atit R, Sgaier SK, Mohamed OA, Taketo MM, Dufort D, Joyner AL*, et al.* (2006) Beta-catenin activation is necessary and sufficient to specify the dorsal dermal fate in the mouse. *Developmental biology* 296:164-76.

Beyer C, Schramm A, Akhmetshina A, Dees C, Kireva T, Gelse K*, et al.* (2012) beta-catenin is a central mediator of pro-fibrotic Wnt signaling in systemic sclerosis. *Annals of the rheumatic diseases* 71:761-7.

Cauchi S, Meyre D, Choquet H, Dina C, Born C, Marre M*, et al.* (2006) TCF7L2 variation predicts hyperglycemia incidence in a French general population: the data from an epidemiological study on the Insulin Resistance Syndrome (DESIR) study. *Diabetes* 55:3189-92.

Cheon SS, Cheah AY, Turley S, Nadesan P, Poon R, Clevers H*, et al.* (2002) beta-Catenin stabilization dysregulates mesenchymal cell proliferation, motility, and invasiveness and causes aggressive fibromatosis and hyperplastic cutaneous wounds. *Proc Natl Acad Sci U S A* 99:6973-8.

Collins CA, Kretzschmar K, Watt FM (2011) Reprogramming adult dermis to a neonatal state through epidermal activation of beta-catenin. *Development* 138:5189-99.

Donati G, Proserpio V, Lichtenberger BM, Natsuga K, Sinclair R, Fujiwara H*, et al.* (2014) Epidermal Wnt/beta-catenin signaling regulates adipocyte differentiation via secretion of adipogenic factors. *Proc Natl Acad Sci U S A* 111:E1501-9.

Driskell RR, Giangreco A, Jensen KB, Mulder KW, Watt FM (2009) Sox2-positive dermal papilla cells specify hair follicle type in mammalian epidermis. *Development* 136:2815-23.

Driskell RR, Juneja VR, Connelly JT, Kretzschmar K, Tan DW, Watt FM (2012) Clonal growth of dermal papilla cells in hydrogels reveals intrinsic differences between Sox2-positive and -negative cells in vitro and in vivo. *J Invest Dermatol* 132:1084-93.

Driskell RR, Lichtenberger BM, Hoste E, Kretzschmar K, Simons BD, Charalambous M*, et al.* (2013) Distinct fibroblast lineages determine dermal architecture in skin development and repair. *Nature* 504:277-81.

Driskell RR, Watt FM (2015) Understanding fibroblast heterogeneity in the skin. *Trends Cell Biol* 25:92-9.

Dulauroy S, Di Carlo SE, Langa F, Eberl G, Peduto L (2012) Lineage tracing and genetic ablation of ADAM12(+) perivascular cells identify a major source of profibrotic cells during acute tissue injury. *Nature medicine* 18:1262-70.

Enshell-Seijffers D, Lindon C, Kashiwagi M, Morgan BA (2010) beta-catenin activity in the dermal papilla regulates morphogenesis and regeneration of hair. *Dev Cell* 18:633-42.

Festa E, Fretz J, Berry R, Schmidt B, Rodeheffer M, Horowitz M*, et al.* (2011) Adipocyte lineage cells contribute to the skin stem cell niche to drive hair cycling. *Cell* 146:761-71.

Fujiwara H, Ferreira M, Donati G, Marciano DK, Linton JM, Sato Y*, et al.* (2011) The basement membrane of hair follicle stem cells is a muscle cell niche. *Cell* 144:577-89.

Gesta S, Tseng YH, Kahn CR (2007) Developmental origin of fat: tracking obesity to its source. *Cell* 131:242-56.

Gupta RK, Arany Z, Seale P, Mepani RJ, Ye L, Conroe HM*, et al.* Transcriptional control of preadipocyte determination by Zfp423. *Nature* 464:619-23.

Hamburg-Shields E, DiNuoscio GJ, Mullin NK, Lafayatis R, Atit RP (2015) Sustained beta-catenin activity in dermal fibroblasts promotes fibrosis by up-regulating expression of extracellular matrix protein-coding genes. *J Pathol* 235:686-97.

Hamilton TG, Klinghoffer RA, Corrin PD, Soriano P (2003) Evolutionary divergence of platelet-derived growth factor alpha receptor signaling mechanisms. *Mol Cell Biol* 23:4013-25.

Harada N, Tamai Y, Ishikawa T, Sauer B, Takaku K, Oshima M*, et al.* (1999) Intestinal polyposis in mice with a dominant stable mutation of the beta-catenin gene. *EMBO J* 18:5931-42.

Haupt A, Thamer C, Heni M, Ketterer C, Machann J, Schick F*, et al.* (2010) Gene variants of TCF7L2 influence weight loss and body composition during lifestyle intervention in a population at risk for type 2 diabetes. *Diabetes* 59:747-50.

Kaushal GS, Rognoni E, Lichtenberger BM, Driskell RR, Kretzschmar K, Hoste E*, et al.* (2015) Fate of Prominin-1 Expressing Dermal Papilla Cells during Homeostasis, Wound Healing and Wnt Activation. *J Invest Dermatol* 135:2926-34.

Kennell JA, MacDougald OA (2005) Wnt signaling inhibits adipogenesis through beta-catenin-dependent and -independent mechanisms. *J Biol Chem* 280:24004-10.

Kretzschmar K, Watt FM (2014) Markers of epidermal stem cell subpopulations in adult mammalian skin. *Cold Spring Harbor perspectives in medicine* 4.

Lichtenberger BM, Mastrogiannaki M, Watt FM (2016) Epidermal [beta]-catenin activation remodels the dermis via paracrine signalling to distinct fibroblast lineages. *Nat Commun* 7.

Lim X, Nusse R (2013) Wnt signaling in skin development, homeostasis, and disease. *Cold Spring Harb Perspect Biol* 5.

Liu S, Herault Y, Pavlovic G, Leask A (2014) Skin progenitor cells contribute to bleomycin-induced skin fibrosis. *Arthritis Rheumatol* 66:707-13.

Longo KA, Wright WS, Kang S, Gerin I, Chiang SH, Lucas PC*, et al.* (2004) Wnt10b inhibits development of white and brown adipose tissues. *J Biol Chem* 279:35503-9.

Marangoni RG, Korman BD, Wei J, Wood TA, Graham LV, Whitfield ML*, et al.* (2015) Myofibroblasts in murine cutaneous fibrosis originate from adiponectin-positive intradermal progenitors. *Arthritis & rheumatology* 67:1062-73.

Millar SE (2002) Molecular mechanisms regulating hair follicle development. *J Invest Dermatol* 118:216-25.

Muller-Rover S, Handjiski B, van der Veen C, Eichmuller S, Foitzik K, McKay IA*, et al.* (2001) A comprehensive guide for the accurate classification of murine hair follicles in distinct hair cycle stages. *J Invest Dermatol* 117:3-15.

Ohgo S, Hasegawa S, Hasebe Y, Mizutani H, Nakata S, Akamatsu H (2013) Bleomycin inhibits adipogenesis and accelerates fibrosis in the subcutaneous adipose layer through TGF-beta1. *Experimental dermatology* 22:769-71.

Ohtola J, Myers J, Akhtar-Zaidi B, Zuzindlak D, Sandesara P, Yeh K*, et al.* (2008) beta-Catenin has sequential roles in the survival and specification of ventral dermis. *Development* 135:2321-9.

Paus R, Muller-Rover S, Van Der Veen C, Maurer M, Eichmuller S, Ling G*, et al.* (1999) A comprehensive guide for the recognition and classification of distinct stages of hair follicle morphogenesis. *J Invest Dermatol* 113:523-32.

Plikus MV, Chuong CM (2014) Macroenvironmental regulation of hair cycling and collective regenerative behavior. *Cold Spring Harbor perspectives in medicine* 4:a015198.

Plikus MV, Mayer JA, de la Cruz D, Baker RE, Maini PK, Maxson R*, et al.* (2008) Cyclic dermal BMP signalling regulates stem cell activation during hair regeneration. *Nature* 451:340-4.

Rinkevich Y, Walmsley GG, Hu MS, Maan ZN, Newman AM, Drukker M*, et al.* (2015) Skin fibrosis. Identification and isolation of a dermal lineage with intrinsic fibrogenic potential. *Science* 348:aaa2151.

Rivers LE, Young KM, Rizzi M, Jamen F, Psachoulia K, Wade A*, et al.* (2008) PDGFRA/NG2 glia generate myelinating oligodendrocytes and piriform projection neurons in adult mice. *Nat Neurosci* 11:1392-401.

Sennett R, Rendl M (2012) Mesenchymal-epithelial interactions during hair follicle morphogenesis and cycling. *Seminars in cell & developmental biology* 23:917-27.

Tsai SY, Sennett R, Rezza A, Clavel C, Grisanti L, Zemla R, *et al.* (2014) Wnt/beta-catenin signaling in dermal condensates is required for hair follicle formation. *Dev Biol* 385:179-88.

Uezumi A, Fukada S, Yamamoto N, Takeda S, Tsuchida K (2010) Mesenchymal progenitors distinct from satellite cells contribute to ectopic fat cell formation in skeletal muscle. *Nature cell biology* 12:143-52.

FIGURE LEGENDS

Figure 1. Localization and isolation of Sca1+ and Sca1- dermal fibroblasts

(a-d, n-q) Sections of P2 back skin from PdgfrαEGFP mice showing expression of nuclear EGFP and immunostaining for (a, b) K14 and PDGFRα, (c, d) Sca1, (n, o) FABP4 and (p, q) Perilipin. b, d, o, and q are enlargements of selected regions of a, c, n and p, respectively. Scale bars: 150 μm. Epi: epidermis; der: dermis; HF: hair follicle; ad: adipocyte; pap: papillary; ret: reticular. (e) Flow cytometry plot showing gating of different dermal subpopulations on the basis of PdgfrαEGFP and Sca1 expression. (f-m) Q-PCR analysis of mRNA levels in sorted cell populations: PdgfrαEGFP-/ Sca1-, PdgfrαEGFP+/ Sca1- and PdgfrαEGFP+/ Sca1+. Genes were normalized to *Gapdh*. Error bars represent SEM of replicates from 4 mice. * p≤0.05; ** p≤0.005; *** p≤0.0005 compared to GFP- cells; $^{\#}$ p≤0.05 compared to EGFP+/ Sca1- cells.

Figure 2. Distinct transcriptional signature of PdgfrαEGFP+/ Sca1+ dermal cells

(a) Heat map showing hierarchical clustering (based on entities and samples) of all differentially regulated entities (p<0.05, fold change >2) between PdgfrαEGFP+/ Sca1+ and PdgfrαEGFP+/ Sca1- fibroblasts. (b) Selected genes upregulated or downregulated in Sca1+ cells. Values in brackets represent fold change of the respective gene. (c) Heat map showing hierarchical clustering (based on entities) of all regulated genes in the Gene Ontology (GO) term 'Wnt receptor signaling pathway'. (d-k) Q-PCR analysis of mRNA levels in sorted cell populations, normalized to *Gapdh*. Error bars represent SEM of replicates from 4 mice. * p≤0.05; ** p≤0.005; *** p≤0.0005 compared to GFP- cells; $^{\#}$ p≤0.05 compared to GFP+/ Sca1- cells. (l, m) Immunofluorescent staining of neonatal skin with an antibody detecting

β-catenin. Red arrow heads depict β-catenin+ fibroblasts in the reticular dermis. DAPI labels nuclei. Scale bar: 200 μm. (n) Section of P1 back skin immunostained for Tcf3/4 (red) and Lef1 (green). Arrowheads indicate double labelled cells. Dashed lines demarcate epidermal-dermal boundary. Scale bar: 100 μm. (o-r) Higher magnification images of the boxed area in the upper (o, q) and lower (p, r) dermis of (m, n).

Figure 3. β-catenin stabilization in dermal fibroblasts via PdgfrαCreER^{T2} (a) Schematic illustration of experimental strategy. (b) Recombination efficiency of PDGFRαCreER^{T2}. Bar graph showing percentage of TdTomato+ cells within different fibroblast subsets after gating for ITGA6-/LIN-/CD31- cells 2 days after 4OHT-mediated recombination via PDGFRαCreER^{T2}. Data show means ± SEM of triplicate samples in a representative experiment (n=2-3 independent experiments). (c, d) TdTomato expression in 4OHT-treated dorsal skin from (c) PDGFRαCreER^{T2} x TdTomato-LSL x Ctnnb1 Exon3$^{+/+}$ (Ctr) and (d) PDGFRαCreER^{T2} x TdTomato-LSL x Ctnnb1 Exon3$^{Flox/+}$ (cΔex3) mice at P4. (e-h) Strong β-catenin staining is detected in TdTomato+ fibroblasts of mice with activated Wnt/β-catenin signaling. Note that the PDGFRαCreER^{T2} transgene is also active in cells of the dermal papilla (DP; red arrow heads in g). White arrow heads in (h) depict β-catenin+ cells in the DP. (i-p) Paraffin sections of back skin of control (Ctr) and mutant (cΔex3) littermates stained for Hematoxylin/Eosin at (i, j) P4, (k, l) first telogen (P18), (m, n) anagen (P35), (o, p) second telogen (P56). Boxed areas in (k, l) are shown as higher magnification inserts. Scale bars: 200μm. (q, r) Hair follicle length measured in male (q) and female (r) cΔex3 and control mice at P4, P11, P18, P24, P28, P35, P42 and P56 (n=2-8). Data points are means ± SEM. (s) Quantification of proliferating, phospho-Histone

H3+ cells in the outer root sheath (ORS) of HF in immunostained skin sections (n= 3 biological samples; ≥5 HF per biological sample were scored).

Figure 4. Induction of dermal fibrosis and proliferation by β-catenin stabilization (a, b) Herovici staining differentiates between immature collagen fibers (blue) versus mature collagen (pink). Note fibrotic region with mature ECM in (b) (boxed). (c) Relative expression of differentiation genes in flow-sorted Tdtomato+ fibroblasts. Data represent mean ± SEM (n=3). * p≤0.05. (d-i) Immunostained paraffin sections of 35 day old mutant and control skin. (j, k) Wholemount thick sections stained for LipidTox (green) with DAPI counterstain (blue). (l, m) Quantification in paraffin sections of P35 skin of (l) adipocytes and (m) EdU+ fibroblasts in the adipocyte layer and interfollicular dermis (including papillary fibroblasts, dermal sheath and reticular fibroblasts). The boundary between papillary/reticular and adipocyte layer was defined by the interface between the bottom of the reticular layer and the upper layer of differentiated adipocytes. Data points are means ± SEM. n≥5 for each group. * p≤0.05; ** p≤0.005; *** p≤0.0005. (n, o) Skin labelled with EdU (green) for 4 hours prior to harvesting, co-stained for Pdgfrα (red), Keratin 14 (white) and DAPI (blue). White arrowheads indicate EdU+ fibroblasts within the adipose layer. Insert is a higher magnification image of the boxed area. Scale bars: 200μm.

Figure 5. β-catenin stabilization in the lower dermis via Dlk1CreER^{T2} (a) Schematic illustration of experimental strategy. (b, c) Quantification of TdTomato+ cells in E18.5 dermal cell suspensions (ITGA6-/LIN-/CD31-) 2 days after 4OHT injection. (b) Percentage of TdTomato+ cells in each fibroblast subpopulation. (c)

Percentage of each fibroblast subpopulation that was TdTomato+. Data show means ± SEM of quadruplicate samples in a representative experiment (n=3 independent experiments). (d, e) TdTomato expressing cells in P56 back skin of Dlk1CreER^{T2} x TdTomato-LSL x Ctnnb1 Exon3$^{+/+}$ (ctr) and Dlk1CreER^{T2} x TdTomato-LSL x Ctnnb1 Exon3$^{Flox/+}$ (Dlk1LTΔex3) mice. Asterisks in (d) demarcate terminally differentiated adipocytes. (f, g) Hematoxylin/Eosin and (h, i) Herovici staining of paraffin sections of P56 ctr and Dlk1LTΔex3 mouse back skin. Arrows in (g, i) indicate fibrotic regions. (j-m) P56 ctr and Dlk1LTΔex3 back skin labelled for β-catenin or caveolin-1 and keratin 14, counterstained with DAPI. Vertical lines indicate thickness of adipocyte layer (AL). Dashed line in (k) demarcates fibrotic tissue (FT). (n, o) Quantification of fibrotic area shown as percentage of the adipocyte layer (n) and adipocytes (o). (p) Quantification of EdU labelled fibroblasts in the interfollicular dermis (including papillary fibroblasts, dermal sheath and reticular fibroblasts) and adipose layer (defined as in Figure 4h) following a 2h EdU pulse. Data show means ± SEM of triplicate samples in a representative experiment (n=3-5). * p ≤0.05; ** p ≤0.005. (q, r) EdU staining of sections shown in (d, e). Scale bars: 200μm.

Figure 6. Effect of β-catenin stabilization on adipocyte differentiation in cultured Sca1+ fibroblasts (a) Schematic illustration of experimental strategy. (b-d) Sca1+/ TdTomato+ targeted fibroblasts from dermal cell suspensions of PDGFRαCreER^{T2} x TdTomato-LSL x Ctnnb1 Exon3$^{+/+}$ (Ctr) and PDGFRαCreER^{T2} x TdTomato-LSL x Ctnnb1 Exon3$^{Flox/+}$ (cΔex3) littermates were isolated by flow cytometry. (b, c) Gating out α6 integrin-positive cells (ITGA6; keratinocytes) (b) and positive selection for Sca1+/ TdTomato+ cells (c). (d) Recombination efficiency (%

TdTomato+ cells) in Cd24+/ Sca1- and Cd24-/ Sca1+ cells. Data show means ± SEM of triplicate samples in a representative experiment (n=3 independent experiments) ns: difference not significant. (e) Examples of individual colonies formed by Sca1+ fibroblasts stained for LipidTox (green), TdTomato (red) and DAPI (blue). Scale bars = 10 μm. (f, g) Percentage of colonies containing 1, 2, 3-5 or more than 5 cells in standard (f) and adipogenic (g) medium. (h, i) Total LipidTox fluorescence (lipid intensity) per clone in control (ctr) and mutant (cΔex3) cultures grown in standard (h) or adipogenic (i) medium. (f-i) n = 2-3 biological replicates and 2 technical replicates. ns: no significant difference; * p≤0.05; ** p≤0.01, *** p≤0.005. f, g: two-way ANOVA with a Bonferroni post-test. h, i: 25% confidence intervals are shown.

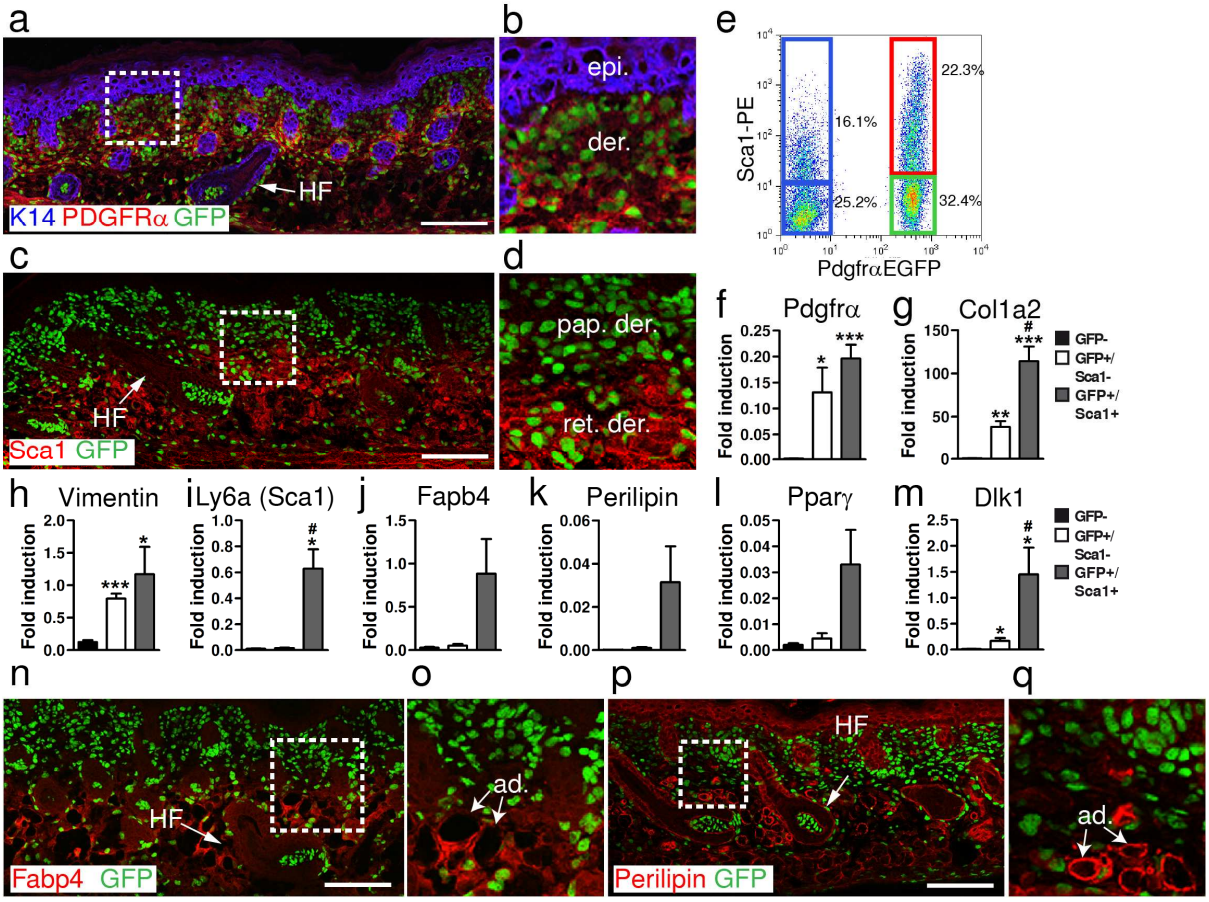

a

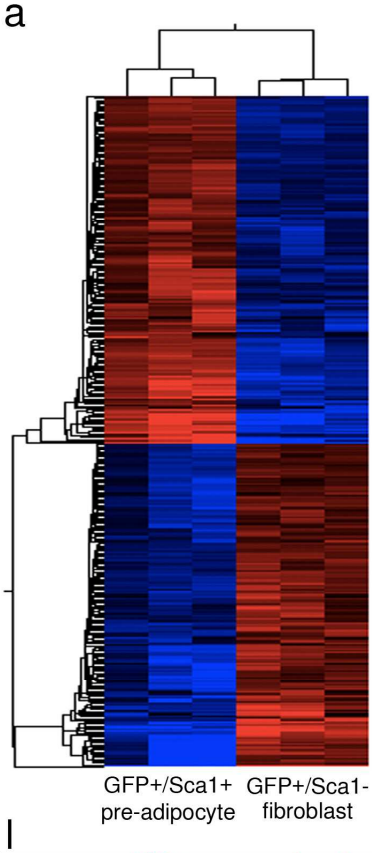

b

	Genes >2 fold upregulated	Genes >2 fold downregulated
Adipogenesis	Fabp4 (7.63), Pparg (5.52), Adipoq(16.13), Lepr (2.49), Dlk1 (6.68), CD36 (10.64), Fbn1 (2.31)	
Wnt signaling	Tcf7l2 (Tcf4; 2.19), Fzd4 (15.12)	Wnt5a (4.86), Lef1 (4.14), Tcf7 (2.43), Axin2 (2.02), Wisp1 (2.97), Dkk1(2.84), Dkk2 (3.35), Frzb (7.05), Fzd3 (2.25), Sostdc1 (2.07), Tle4 (2.91), Nkd2 (2.11)
BMP signaling	Bmper (27.15)	Bmp4 (3.76), Bmp7 (4.74)
Notch signaling		Hey1 (6.23), Hey2 (5.13), Hes5 (13.11), Dll1 (7.21)
PDGF signaling	Pdgfrl (2.28)	Pdgfa (2.02), Pdgfc (2.25)
Zinc finger proteins	Zfp385a (3.47), Zfp462 (2.25)	Zfp238 (2.42), Zfp711 (2.01), Zfp365 (3.02), Zfp618 (2.27)

c

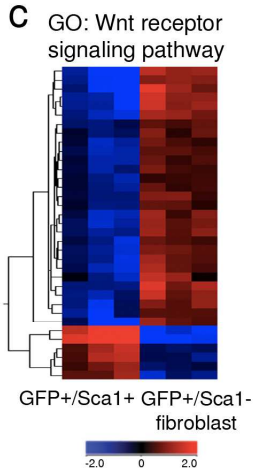

d

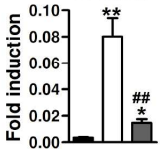

e

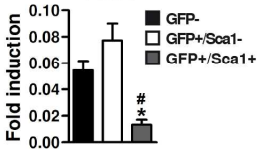

f

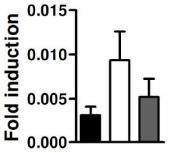

g

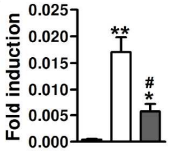

h

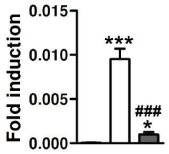

i

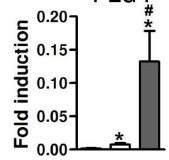

j

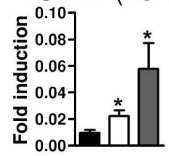

k

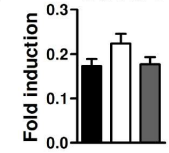

l

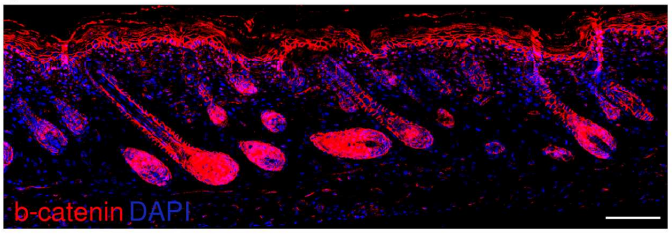

m

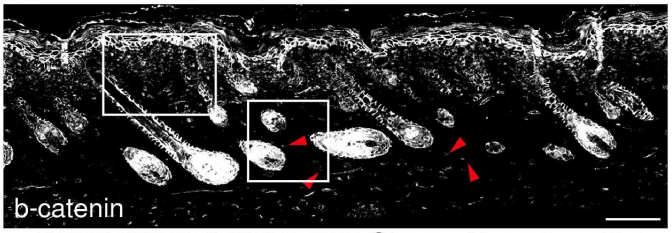

n

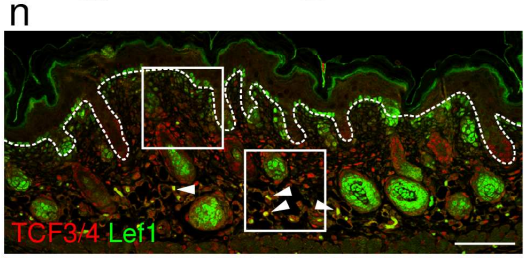

o

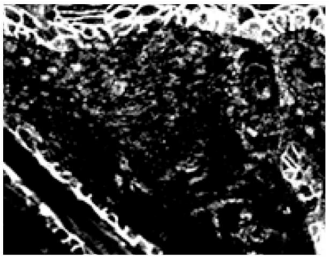

p

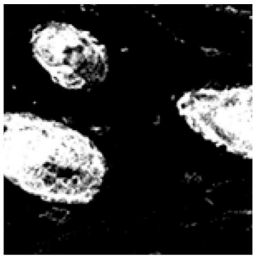

q

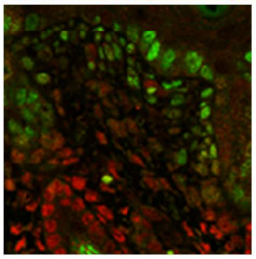

r

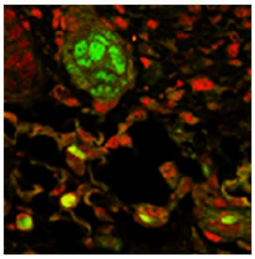

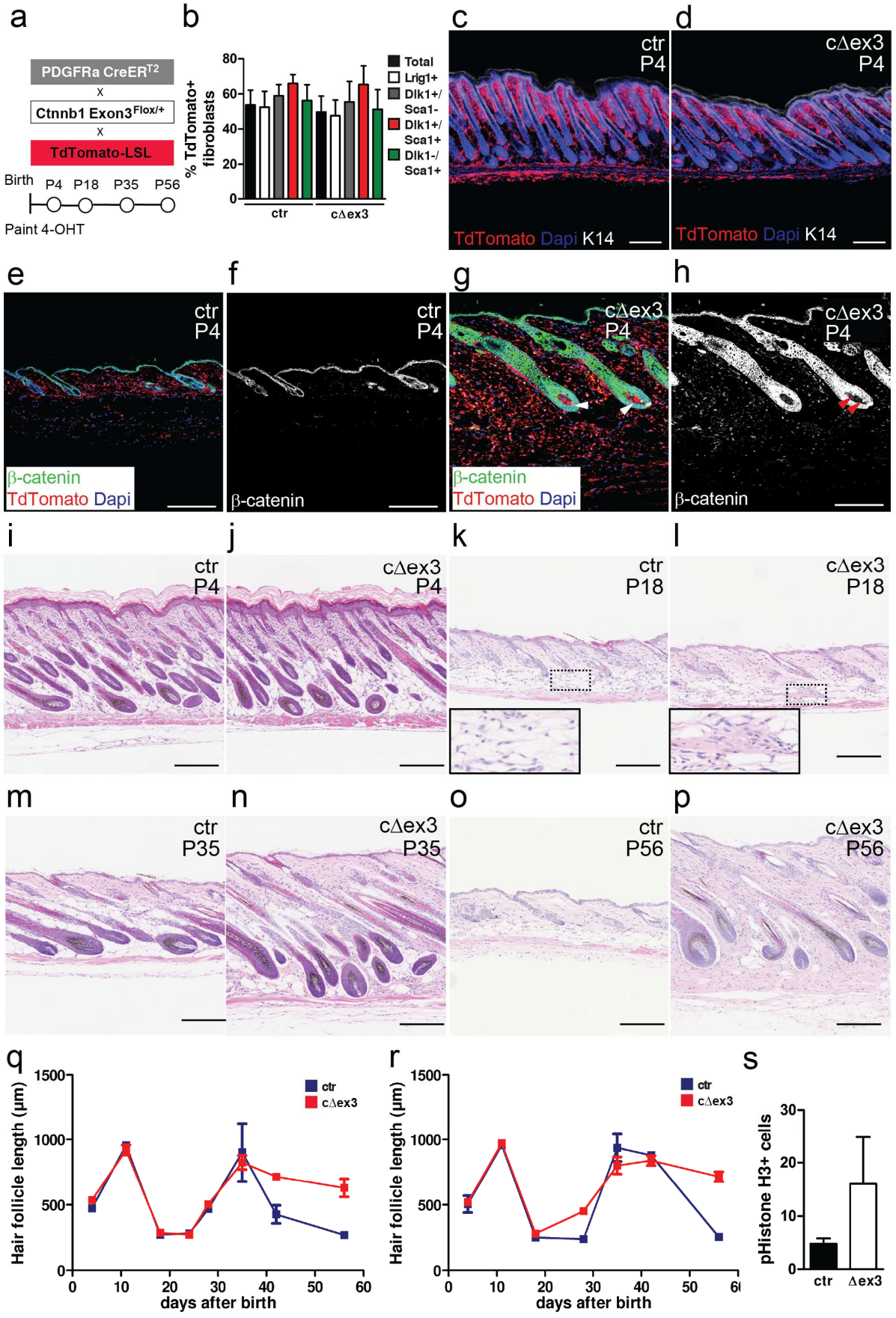
a
PDGFRa CreER^{T2}
x
Ctnnb1 Exon3$^{Flox/+}$
x
TdTomato-LSL
Birth P4 P18 P35 P56
Paint 4-OHT
b
% TdTomato+ fibroblasts
Total
Lrig1+
Dlk1+/ Sca1-
Dlk1+/ Sca1+
Dlk1-/ Sca1+
ctr
cΔex3
c
ctr P4
TdTomato Dapi K14
d
cΔex3 P4
TdTomato Dapi K14
e
ctr P4
β-catenin TdTomato Dapi
f
ctr P4
β-catenin
g
cΔex3 P4
β-catenin TdTomato Dapi
h
cΔex3 P4
β-catenin
i
ctr P4
j
cΔex3 P4
k
ctr P18
l
cΔex3 P18
m
ctr P35
n
cΔex3 P35
o
ctr P56
p
cΔex3 P56
q
Hair follicle length (μm)
ctr
cΔex3
days after birth
r
Hair follicle length (μm)
ctr
cΔex3
days after birth
s
pHistone H3+ cells
ctr
Δex3

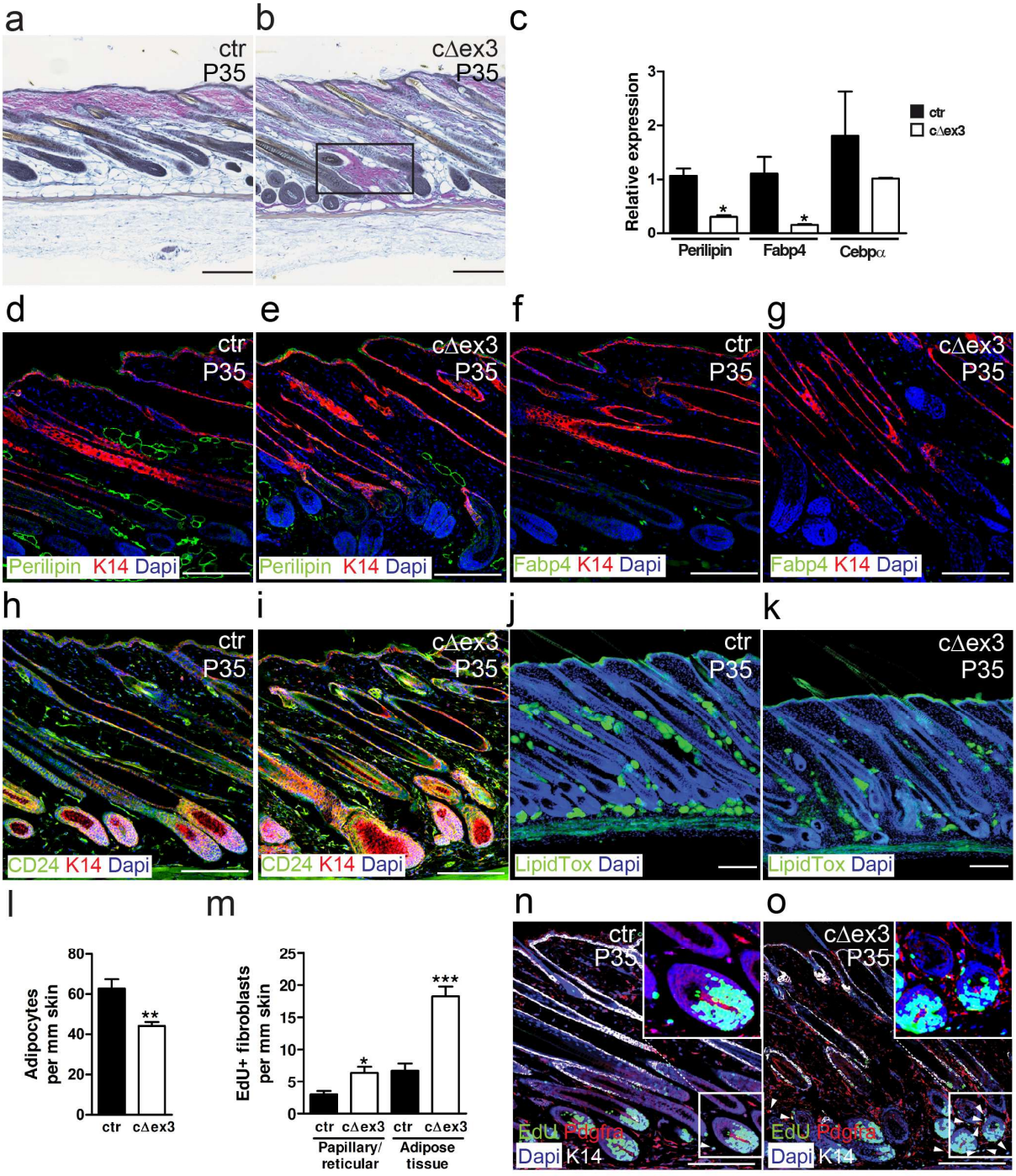
a
ctr
P35
b
cΔex3
P35
c
Relative expression
ctr
cΔex3
Perilipin
Fabp4
Cebpα
d
Perilipin K14 Dapi
e
Perilipin K14 Dapi
f
Fabp4 K14 Dapi
g
Fabp4 K14 Dapi
h
CD24 K14 Dapi
i
CD24 K14 Dapi
j
LipidTox Dapi
k
LipidTox Dapi
l
Adipocytes per mm skin
m
EdU+ fibroblasts per mm skin
Papillary/ reticular
Adipose tissue
n
EdU Pdgfra Dapi K14
o
EdU Pdgfra Dapi K14

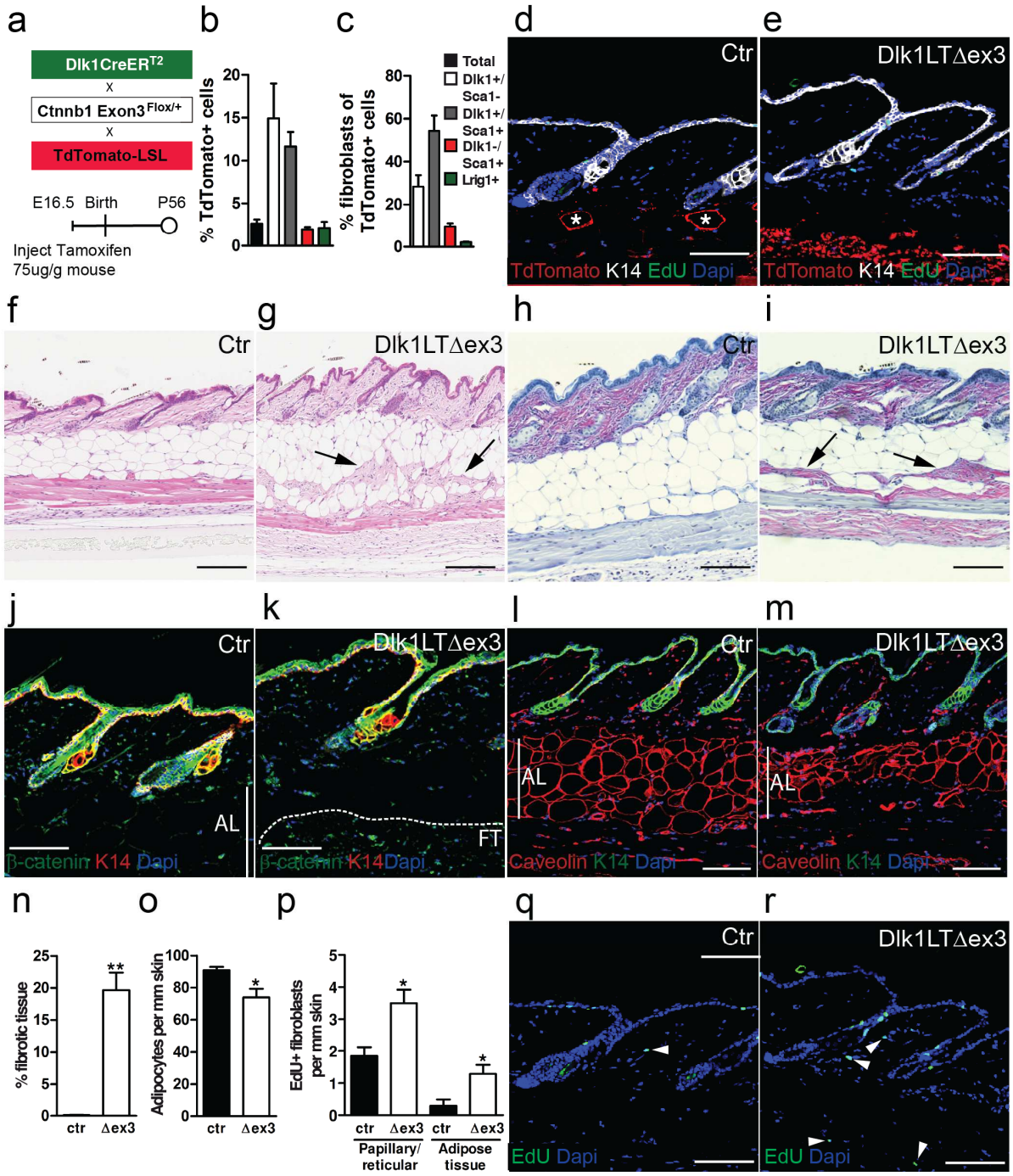
a
Dlk1CreER^T2
x
Ctnnb1 Exon3^Flox/+
x
TdTomato-LSL
E16.5 Birth P56
Inject Tamoxifen
75ug/g mouse
b
% TdTomato+ cells
c
% fibroblasts of TdTomato+ cells
Total
Dlk1+/ Sca1-
Dlk1+/ Sca1+
Dlk1-/ Sca1+
Lrig1+
d
Ctr
TdTomato K14 EdU Dapi
e
Dlk1LTΔex3
TdTomato K14 EdU Dapi
f
Ctr
g
Dlk1LTΔex3
h
Ctr
i
Dlk1LTΔex3
j
Ctr
AL
β-catenin K14 Dapi
k
Dlk1LTΔex3
FT
β-catenin K14Dapi
l
Ctr
AL
Caveolin K14 Dapi
m
Dlk1LTΔex3
AL
Caveolin K14 Dapi
n
% fibrotic tissue
ctr Δex3
o
Adipocytes per mm skin
ctr Δex3
p
EdU+ fibroblasts per mm skin
ctr Δex3 ctr Δex3
Papillary/ reticular
Adipose tissue
q
Ctr
EdU Dapi
r
Dlk1LTΔex3
EdU Dapi

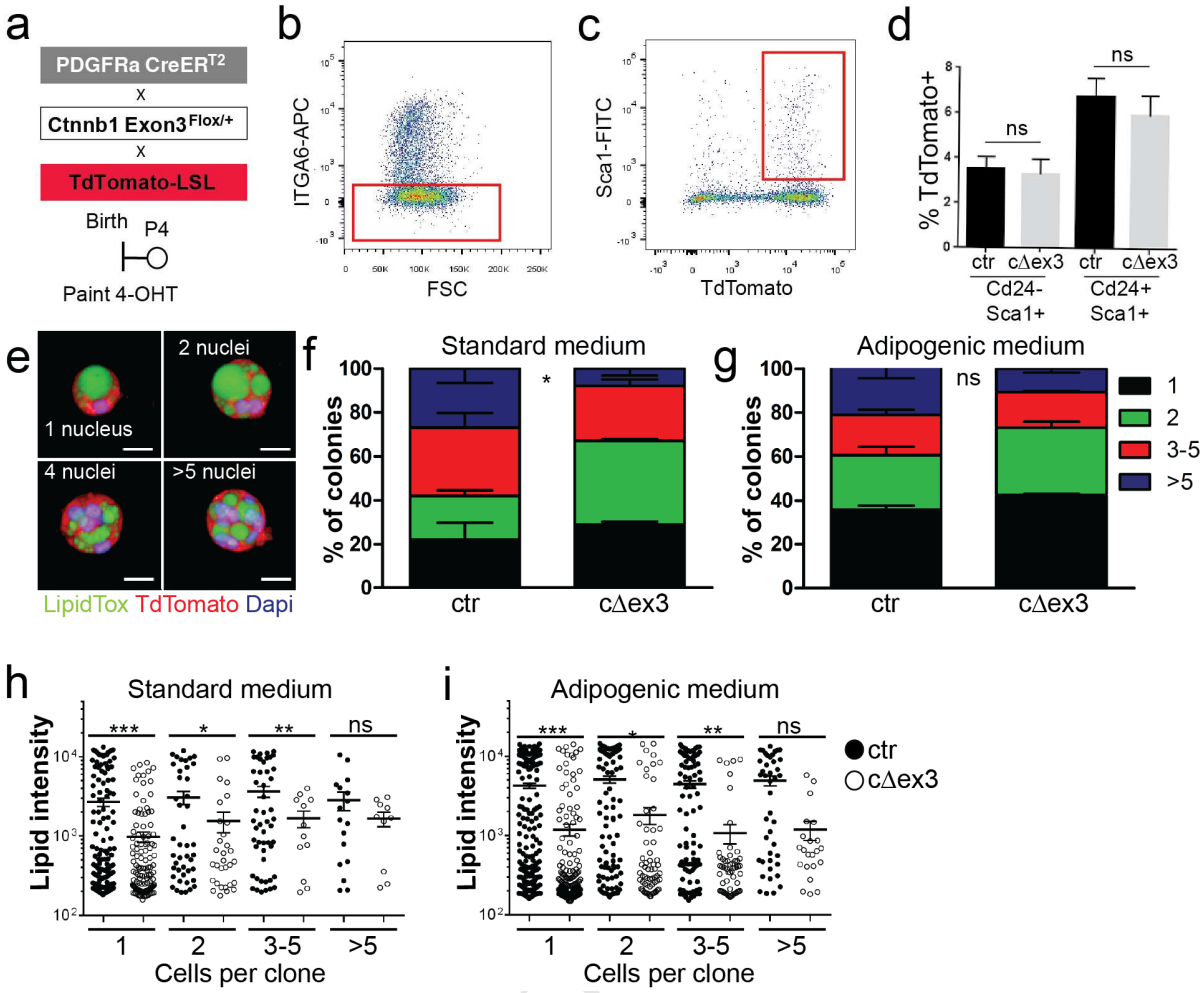
a
PDGFRa CreER^{T2}
x
Ctnnb1 Exon3$^{Flox/+}$
x
TdTomato-LSL
Birth
P4
Paint 4-OHT
b
ITGA6-APC
FSC
c
Sca1-FITC
TdTomato
d
% TdTomato+
ns
ns
ctr
cΔex3
ctr
cΔex3
Cd24-
Sca1+
Cd24+
Sca1+
e
1 nucleus
2 nuclei
4 nuclei
>5 nuclei
LipidTox TdTomato Dapi
f
Standard medium
% of colonies
*
ctr
cΔex3
g
Adipogenic medium
% of colonies
ns
ctr
cΔex3
1
2
3-5
>5
h
Standard medium
Lipid intensity
***
*
**
ns
1
2
3-5
>5
Cells per clone
i
Adipogenic medium
Lipid intensity
***
*
**
ns
ctr
cΔex3
1
2
3-5
>5
Cells per clone